

Available online at [www.sciencedirect.com](http://www.sciencedirect.com)**ScienceDirect**

Physics Procedia 83 (2016) 1083 – 1093

Physics

**Procedia**9<sup>th</sup> International Conference on Photonic Technologies - LANE 2016

## Gas-tight thermally joined metal-thermoplastic connections by pulsed laser surface pre-treatment

André Heckert<sup>a,\*</sup>, Christian Singer<sup>b</sup>, Michael F. Zaeh<sup>a</sup>, Ruediger Daub<sup>b</sup>, Tobias Zeilinger<sup>b</sup><sup>a</sup>*Institute for Machine Tools and Industrial Management (iwb), Technische Universität München, Boltzmannstrasse 15, 85748 Garching, Germany*<sup>b</sup>*BMW Group, Manufacturing Technologies and Prototype Shop Electric Energy Storage, Taunusstrasse 41, 80807 München, Germany*

---

### Abstract

Thermal joining of laser-structured metals and thermoplastics has been proven to deliver a high joint strength. A novel idea is to apply this process onto metal-thermoplastic joints in order to produce gas-tight hybrid connections which can be used in several technical applications.

The surface pre-treatment of aluminum by infrared pulsed laser radiation was focused in this study. Depending on different cumulative energies two main surface topologies, stochastic and deterministic groove structures, were manufactured. Consequently, heat conduction joining by infrared laser radiation was used to join the metal with polypropylene. The influence of laser structuring on surface roughness and groove geometry was analyzed by scanning electron and laser scanning microscopy. The wetting of the thermoplastic was investigated by optical microscopy. The gas-tightness was identified by a helium leak test and climate testing was performed to analyze the long-term durability. The results indicate that depending on the surface morphology of the metal, durable gas-tight connections can be created by thermal joining.

© 2016 The Authors. Published by Elsevier B.V. This is an open access article under the CC BY-NC-ND license (<http://creativecommons.org/licenses/by-nc-nd/4.0/>).

Peer-review under responsibility of the Bayerisches Laserzentrum GmbH

*Keywords:* Thermal joining; thermoplastic metal hybrids; laser surface pre-treatment; gas-tight joint

---

### 1. Motivation and state of the art

Laser-based thermal joining of metal and thermoplastics, also known as LAMP joining (Laser Assisted Metal and Plastic joining), was introduced by Kawahito et al. (2006). The connection between the joining partners is generated

---

\* Corresponding author. Tel.: +49-89-289-1558 .

E-mail address: [andre.heckert@iwb.tum.de](mailto:andre.heckert@iwb.tum.de)

by melting the plastic through a heat input into the metal joint and the following wetting with the metal surface. The joining method can be seen as a fast, flexible, and reliable process to connect the two different materials (Cenigaeonaidia et al. 2012).

To achieve high joint qualities, a surface pre-treatment of the metal is vital (Heckert and Zaeh 2014). Several researchers used a laser surface pre-treatment on the metal with pulsed laser radiation for enhancing the mechanical properties of the hybrid joint. Current work has shown that joint strengths comparable to those by an electrochemical surface pre-treatment such as anodizing and etching can be achieved with laser-surface-pre-treatment (Kurtovic 2014; Rechner 2012; Spadarao et al. 2007, Lamberti et al. 2014). For processing the metal surface with pulsed laser radiation, two different methods exist. On the one hand, the laser pulses are uniformly arranged in an overlapping configuration. By melting, evaporation and the resulting vapour pressure, a chaotic microscopic melt structure is achieved which is characterized by a series of spherical (melt) drops. The dimensions of those stochastic structures are usually smaller than the spot diameter of the laser beam. Amongst the authors using such stochastic structures are Rechner (2012), Hose (2008), Kurtovic (2014), and Heckert and Zaeh (2014). On the other hand, the pulsed laser radiation is used to manufacture deterministic structures like grooves or holes. The dimensions of those structures are in the range of the laser spot diameter or above and the structure geometries are defined. Groove structures were manufactured by Amend et. al. (2013), Amend et. al. (2014), Rodríguez et. al. (2014), and Schricker et al. (2015).

Yet, the research is focused on the improvement of the mechanical strength between metal and plastic. However, for several technical applications other joint properties such as the seal tightness against fluids or gases can be of importance. Roesner (2014) achieved a tightness against permanent immersion in water by joining tubular steel parts with deterministic laser surface structures to polycarbonate covers. Since very little is known concerning seal tightness, the gas-tightness for metal-plastic joints achieved by pulsed laser surface pre-treatment is analyzed in this study.

## 2. Experimental setup

### 2.1. Materials

Aluminum (AL) alloy of the type EN AW-1050A was used as the metal joining partner. The material is characterized by good formability and low mechanical strength. For thermal joining with a thermoplastic material, natural polypropylene (PP) was chosen. PP is characterized by a low water permeability and chemical stability (Saechtling 2007) as well as a low price. Further technical properties of the materials are listed in Table 1.

Table 1. Material properties of aluminum and natural polypropylene.

Parameter	Unit	EN-AW-1050A	PP
Density	g/cm <sup>3</sup>	2.7	0.9
Tensile strength	MPa	32	65
Thermal expansion coefficient	K <sup>-1</sup>	23.5*10 <sup>-6</sup>	1.6*10 <sup>-4</sup>

### 2.2. Laser surface structuring of the aluminum

The surface pre-treatment of the AL specimens was done by using a pulsed single-mode Yb-fibre laser. The specifications of the laser system are a mean output power of 20 W, a wavelength of 1064 nm, and a pulse width of 100 ns. For all specimens, the laser beam was focused to a spot diameter of about 50 µm onto the metal surface. All metal specimens were structured in ambient atmosphere.

Two different surface structures have been manufactured. Firstly, stochastic structures were created by overlapping the pulses in the focal plane in both dimensions (Fig. 1 a).

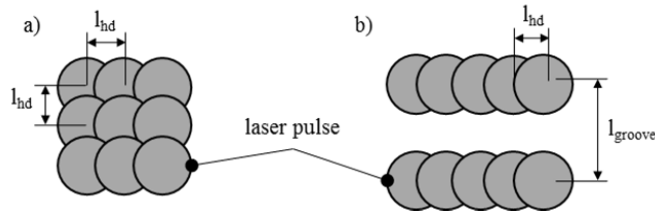


Fig. 1. Schematic illustration of the process strategy for (a) stochastic and (b) groove structures.

The hatch distance  $l_{hd}$  was varied between 10  $\mu\text{m}$  and 30  $\mu\text{m}$ . The stochastic structures were evaluated based on the cumulative laser energy  $E_{cum,S}$  irradiated to the surface.  $E_{cum,S}$  was defined by the pulse energy  $E_p$ , the hatch distance  $l_{hd}$  and the number of repetitions  $n_{rep}$ :

$$E_{cum,S} = \frac{4 \cdot E_p}{\pi \cdot l_{hd}^2} \cdot n_{rep} \tag{1}$$

Secondly, a groove structure was generated by applying a parallel line pattern (Fig. 1 b). The line distance  $l_{groove}$  was defined to be 100  $\mu\text{m}$ . The grooves were manufactured by overlapping laser pulses in the direction of the laser feed motion. The laser parameters were varied in terms of the cumulative energy  $E_{cum,G}$ :

$$E_{cum,G} = \frac{E_p}{l_{hd}} \cdot n_{rep} \tag{2}$$

The utilized laser parameters for the surface pre-treatment are listed in Table 2.

Table 2. Laser parameters for surface pre-treatment of aluminum for the stochastic and the groove structure.

Parameter	Unit	Stochastic structure								Groove structure				
		0.5	1.0	0.5	1.0	1.0	1.0	1.0	1.0	1.0	1.0	1.0	1.0	1.0
Pulse energy	mJ	0.5	1.0	0.5	1.0	1.0	1.0	1.0	1.0	1.0	1.0	0.5	1.0	1.0
Hatch distance	$\mu\text{m}$	20	30	20	20	20	10	10	20	20	30	10	10	10
Repetitions	-	1	2	4	2	4	1	2	2	5	10	10	5	10
Cumulative energy	$\text{J}/\text{cm}^2$	159	283	636	636	1273	1273	2546	1.0	2.5	3.3	5.0	5.0	10.0

### 2.3. Thermal joining of the laser structured specimens and mechanical test

Bonding of AL and PP was performed by laser-based heat conduction joining. For this purpose, the specimens were clamped and compressed by a force of 175 N. The AL was irradiated by a single-mode Yb-fibre laser to heat the metal and to melt the PP. A scanning optics was used to apply laser trajectories according to Fig. 2. Two different types of joints were manufactured. Firstly, the tensile shear strength in dependence of the surface structure was analyzed. In order to do that, AL and PP specimens were joined as illustrated in Fig. 2 (a) and tested according to DIN EN 1645:2009. A laser power of 1200 W, a feed rate of 0.5 m/s and 165 repetitions of the trajectory were used for the joining process. Secondly, cylindrical PP specimens were joined to tubular AL parts as shown in Fig. 2 (b). The AL specimens exhibit a gas reservoir including two holes. One hole was sealed by the PP and utilized for the gas-tightness test. The remaining filling neck was connected with the measuring equipment. The PP was joined with a heat input achieved by a laser power of 1000 W, a feed rate of 1.0 m/s and a circular trajectory with 500 repetitions.

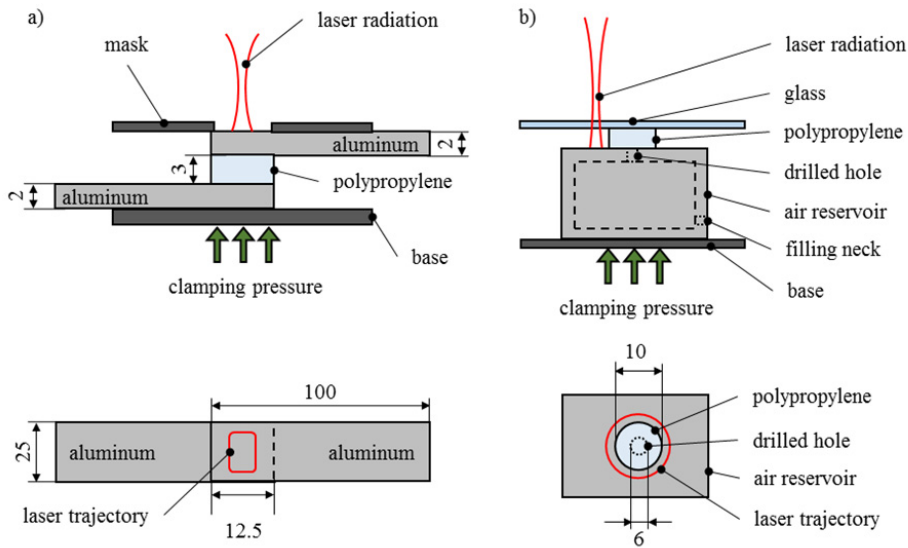


Fig. 2. Thermal joining of specimens for (a) tensile shear strength test and (b) gas-tightness test.

Three specimens of each laser surface structure were manufactured to test the gas-tightness. The tensile shear strength was calculated from the breaking force divided by the overlapping area. Six samples of each type of laser surface structure were used to calculate an average joint strength, whereby either three specimens were fractured right after joining or used for long-term durability testing. The long-term durability was analyzed by a climate change test referring to the internal standard BMW PR308.2. This cycle included a warm-up to 85 °C for one hour at an atmospheric moisture of 80 % as well as a cooling phase to -40 °C. The dwell time for both temperatures was defined to be two hours. The specimens were stored in the climate testing laboratory for ten cycles.

#### 2.4. Surface analyses for the laser structured aluminum

An analysis of the laser structured surface topography was carried out by scanning electron microscopy (SEM), laser scanning microscopy (LSM), and optical microscopy.

SEM was used to identify re-solidified molten material which led to undercuts and a cleft surface depending on the laser processing parameters. Furthermore, the structures were evaluated regarding the formation of oxide. In addition, LSM was utilized to analyse the surface topology. The measuring method allows the generation of a three-dimensional model of the AL surface topology. As a consequence, the mean roughness index  $R_a$  of the stochastic structures was calculated. The groove structures were characterized regarding the groove depth  $d_{\text{groove}}$ , groove width  $w_{\text{groove}}$  and burr height  $h_{\text{burr}}$  as shown in Fig. 3 by both LSM and optical microscopy. Polished micrograph sections of the manufactured joints were utilized for the investigation of the PP-wettability.

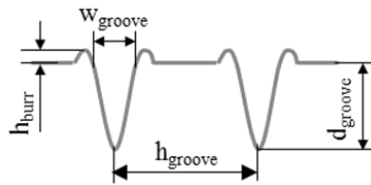


Fig. 3. Schematic illustration of groove structures and definition of groove depth.

### 2.5. Gas-tightness test

The gas-tightness of the hybride AL-PP joints was identified by a helium leak test referring to DIN EN 1779:1999. Due to the smallest atomic radius of all chemical elements, leak tests with helium detect a minimum leakage of approximately  $10^{-10}$  Pa·m<sup>3</sup>/s (DIN EN 1779). Gas tightness of the hybrid metal-thermoplastic joints was defined at a maximum leakage of  $5 \cdot 10^{-7}$  mbar/s. For leakage testing, the specimens with the air reservoir (Fig. 2 b) were placed in the vacuum chamber as shown in Fig. 4. After evacuating the chamber, helium was loaded to the inside of the reservoir. In case of cracks, pores or holes in the joint region, helium leaks from the inside of the reservoir which is then identified by a mass spectrometer.

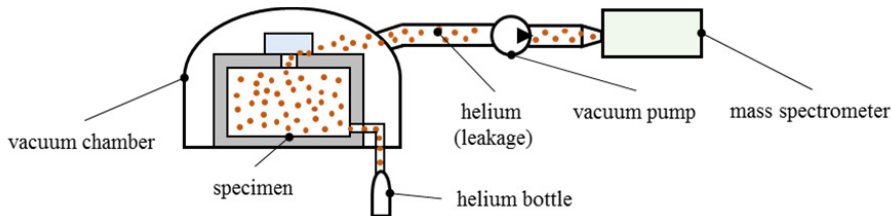


Fig. 4. Identification of gas-tightness by helium leakage test.

## 3. Results and discussion

### 3.1. Analysis of the aluminum surface topology and wetting with the polypropylene

The laser structured AL surfaces with stochastic and groove structures were examined by SEM as shown in Fig. 5. The SEM images display a cleft and rough surface topography for a stochastic structure depending on the amount of cumulative energy. Increasing the energy by higher pulse energy, multiple repetitions or a smaller hatch distance caused a more cleft surface with many undercuts. Especially in case of a low energy amount, less motion of the molten material occurred and the material re-solidified in slightly flatter structures as shown in Fig. 5 (a, b). In contrast, round and nodular melt structures occur when applying high cumulative energies, as shown in Fig. 5 (c).

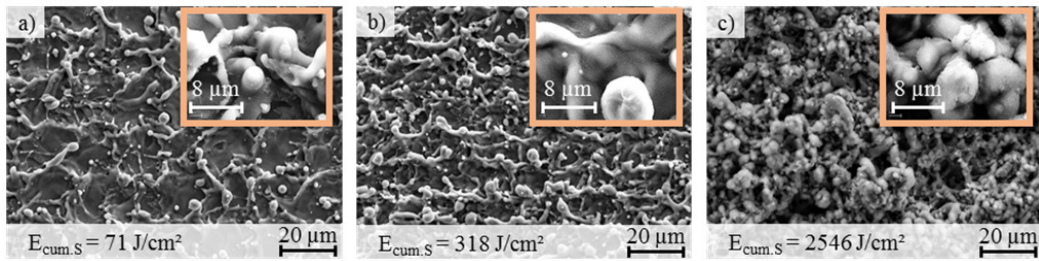


Fig. 5. SEM photographs of aluminum surfaces with stochastic structures for  $E_{cum,S}$  of (a) 71 J/cm<sup>2</sup>; (b) 318 J/cm<sup>2</sup> and (c) 2546 J/cm<sup>2</sup>.

Furthermore, the SEM images show an increasing content of porous oxide on the stochastic structures. The oxide can be identified as a fuzzy layer. Low cumulative energy caused less formation of oxide. A thick oxide layer was identified for the AL specimens which were pre-treated with a higher cumulative energy (Fig. 5 c). The findings are in accordance to Rechner 2012, Hose 2008 and Kurtovic 2014.

The SEM images of the groove structures (Fig. 6) illustrate an increase in structure depth depending on the cumulative energy. The material was mainly vaporised by the laser radiation. In addition, re-solidified melt was identified in the structures, which led to a rough surface topology inside the grooves. Some liquified material re-solidified as a burr along the grooves on the surface. While increasing the amount of energy, the formation of the burr increased as it is shown in Fig. 6 (a) to (c). In comparison to the stochastic structures, less oxide was identified.

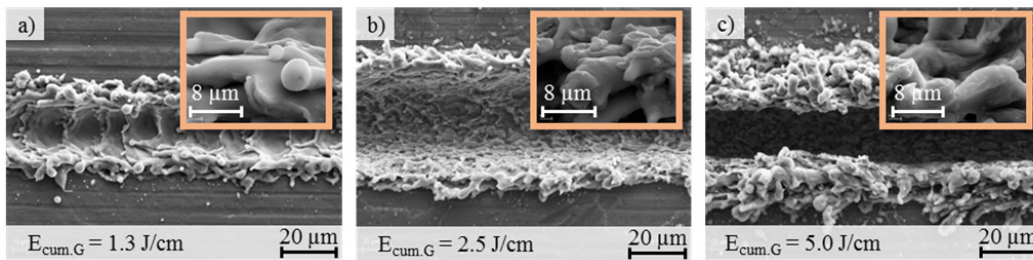


Fig. 6. SEM photographs of aluminum surfaces with groove structures for  $E_{cum,G}$  of (a) 1.3 J/cm; (b) 2.5 J/cm and (c) 5.0 J/cm.

The results for the mean roughness index  $R_a$  of the stochastic structures in dependence of the laser energy are shown in Fig. 7 (a). The values were calculated by an average of five roughness lines along the surface. Each graph in the plot is associated with a specific pulse energy and hatch distance. A minimum mean roughness index of 1.4  $\mu\text{m}$  was measured for a cumulative energy of about 71 J/cm<sup>2</sup> at a pulse energy of 0.5 mJ, a hatch distance of 30  $\mu\text{m}$  and one repetition. Increasing the number of repetitions or the pulse energy as well as lowering the hatch distance caused a higher surface roughness. The mean roughness index for example could be increased by up to 4.0  $\mu\text{m}$  at a pulse energy of 0.5 mJ, a hatch distance of 10  $\mu\text{m}$  and four repetitions. A further increase occurred at a pulse energy of 1.0 mJ which caused a mean roughness index of 4.2  $\mu\text{m}$  when using four repetitions (1273 J/cm<sup>2</sup>). The increase in cumulative energy causes more molten and vaporised material which leads to a higher melting flow and a more cleft surface topology. The mean roughness of up to 8.6  $\mu\text{m}$  was achieved at 5093 J/cm<sup>2</sup> for a pulse energy of 1.0 mJ, a hatch distance of 10  $\mu\text{m}$  and four repetitions.

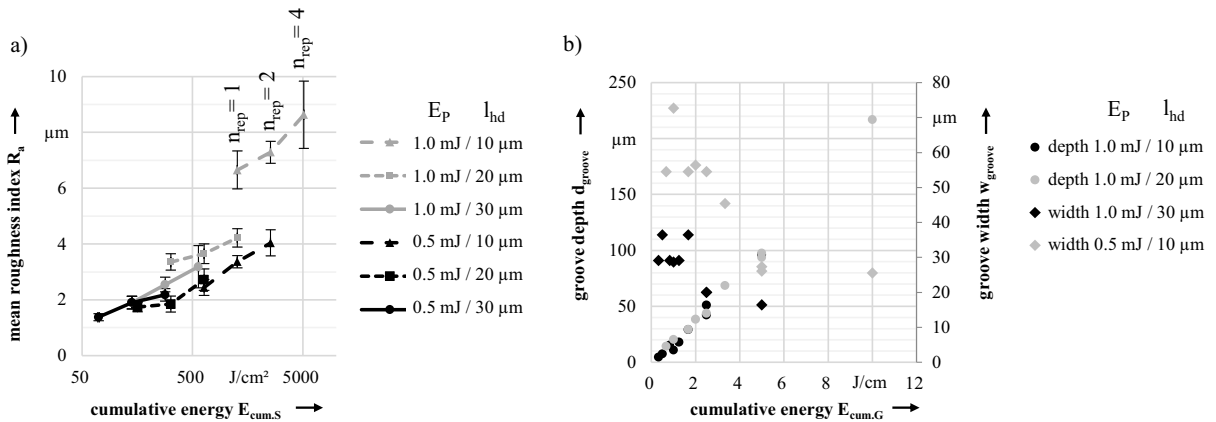


Fig. 7. Mean roughness index  $R_a$  (a) of stochastic structures; (b) groove depth and width of groove structures.

According to the results of Amend et. al. (2013 and 2014) and Rodriguez et. al. 2014, the structure depth of the grooves depends on the cumulative energy. As shown in Fig. 7 (b) and Fig. 8 (a to e) the depth increased linearly by up to approximately 217  $\mu\text{m}$  for the highest cumulative energy. Applying different processing parameters with the same cumulative energy caused almost identical results for the groove depth. For example a structure depth of approximately 95  $\mu\text{m}$  was achieved for a cumulative energy of 5.0  $\text{J}/\text{cm}$  as shown in Fig. 8 (c) and (d). Yet, the aluminum specimens which were pre-treated with a laser pulse energy of 0.5 mJ showed more re-solidified material remains in the groove which led to reduced groove widths (Fig. 8 c). In general, the groove width decreases with the structure depth and is smaller for low pulse energies (Fig. 7 b). For some processing parameters, even a closure of the groove was observed. Furthermore, certain structures exhibited a burr which formed an undercut (Fig. 8 c to d). This effect could be useful in the sense of mechanical interlocking and gas-tightness with the thermoplastic. The burr increased up to a height of about 35  $\mu\text{m}$  for a cumulative energy of 10.0  $\text{J}/\text{cm}$ .

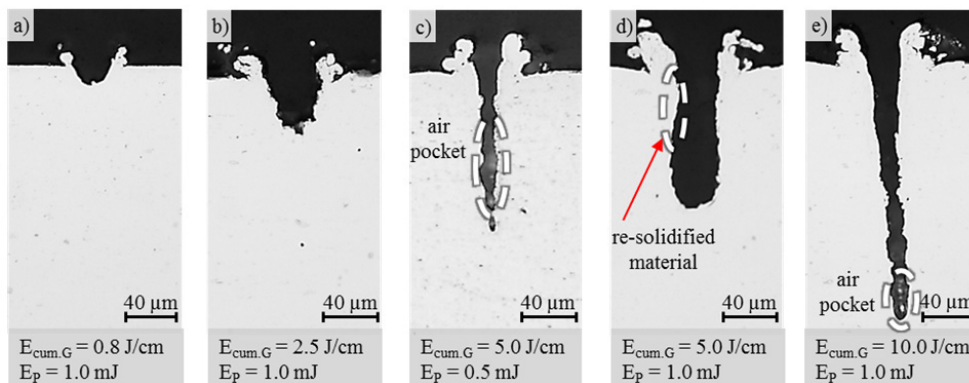


Fig. 8. Groove structures and wetting of polypropylene depending on the cumulative energy  $E_{\text{cum},G}$ .

The groove structures which were manufactured with a pulse energy of 1.0 mJ show a full wetting for a structure depth up to 100  $\mu\text{m}$  (Fig. 8 a, b and d). The PP wets the AL surface without the formation of air pockets, which is considered to be due to the wide structures. Yet, the joined specimens with a groove depth of less than 20  $\mu\text{m}$  were not suitable for further investigations because of a lack in joint strength – the PP was detached from the AL with the slightest mechanical influence. As a consequence of low structure widths, groove structures which were manufactured by a pulse energy of 0.5 mJ showed some air pockets even for depths below 100  $\mu\text{m}$ . Furthermore, the specimens with a structure depth of more than 200  $\mu\text{m}$  (10  $\text{J}/\text{cm}$ ) showed significant air pockets at the bottom of the

grooves (Fig. 8 e).

The formation of air pockets in between the PP and the stochastic structures was influenced by the surface roughness. Fig. 9 shows the air pockets in dependence of the cumulative energy. Low mean roughness values led to no or only a few and very small air pockets as shown in Fig. 9 (a). Increasing the amount of energy and the surface roughness caused larger air pockets (Fig. 9 b and c). As a consequence, the highly clefted surfaces for such cumulative energies hinder the uniform wetting of the AL surface by the PP.

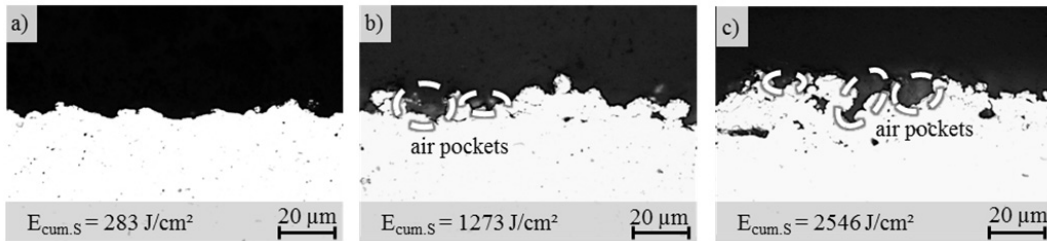


Fig. 9. Stochastic structures and wetting of polypropylene depending on cumulative energy  $E_{cum,M}$ .

### 3.2. Gas-tightness of the hybrid joints

The results for the gas-tightness tests are summarized and shown in Fig. 10, sorted by the cumulative energy and the structure type. Gas-tightness was not achieved for AL-PP joints with stochastically structured specimens with a cumulative energy of 159 J/cm², 283 J/cm², or 636 J/cm² (0.5 mJ). A significant helium leakage mainly after the climate change test was shown for those joints. This could be caused by a lack in wetting and the thermal expansion coefficient which is approximately 7 times larger for the thermoplastic than for the aluminum. Due to the air humidity, it is possible that water molecules accumulated in the joint region.

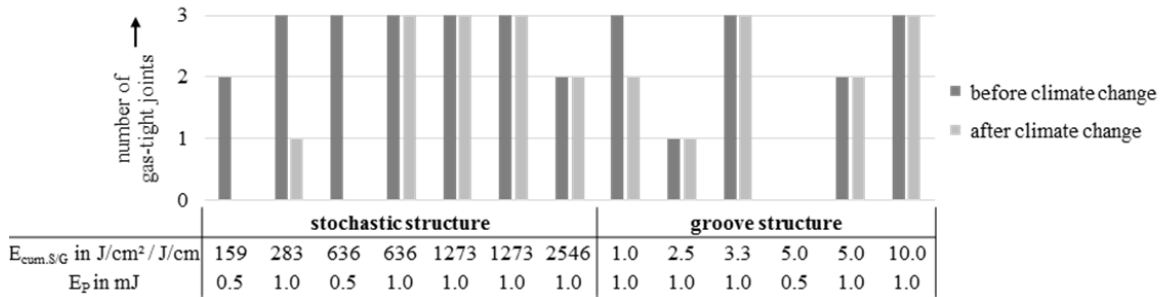


Fig. 10. Gas-tightness of aluminum-polypropylene joints depending on surface structure and cumulative energy.

Specimens with a stochastic structure manufactured at a pulse energy of 1.0 mJ and a cumulative energy above 636 J/cm² were gas-tight (Fig. 10 and 11 a). For those specimens the PP fully wetted the AL surface without the formation of large air pockets. Gas-tightness was therefore given before and after the climate change tests because of sufficient mechanical and specific adhesion between the joining materials. The thermoplastic wetted the metal surface with the formation of very small and spatially separated air pockets for a cumulative energy of 2546 J/cm² (Fig. 11 b), which had no effect on the gas-tightness. Only one joint was leaking due to incomplete wetting of the PP during the thermal joining process, as shown in Fig. 11 (c).



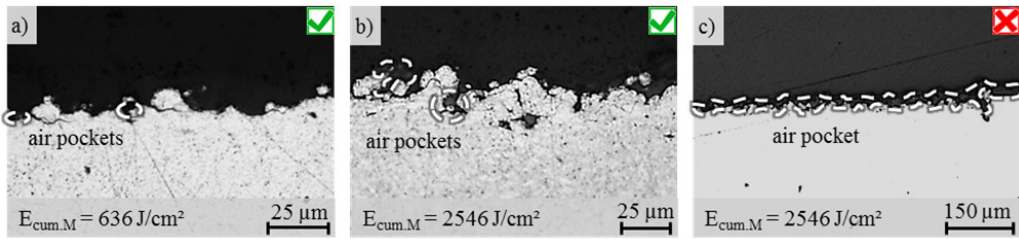


Fig. 11. Cross section images of gas-tight (a and b) and helium leaking (c) joints with stochastic structures with air pockets.

The groove structures manufactured with a pulse energy of 0.5 mJ (5.0 J/cm) caused a gas leakage. This can be referred to the low structure widths of 16 µm. As mentioned before, an incomplete infiltration of the grooves led to a helium leakage along the air pockets in the groove structures. In addition, the thermoplastic could be removed from the metal by applying a slight force. Some of the specimens with a cumulative energy of less than 2.5 J/cm (Fig. 12 a) were indicated as leaking. The joints were gas-tight with a cumulative energy of more than 3.3 J/cm at a pulse energy of 1.0 mJ, as shown in Fig. 10 and 12 (b). The grooves with a structure depth of more than 95 µm were almost fully filled with PP as it is shown in the cross section images in Fig. 12 (c) and (d). Thereby, only a small number of spatially separated air pockets was identified.

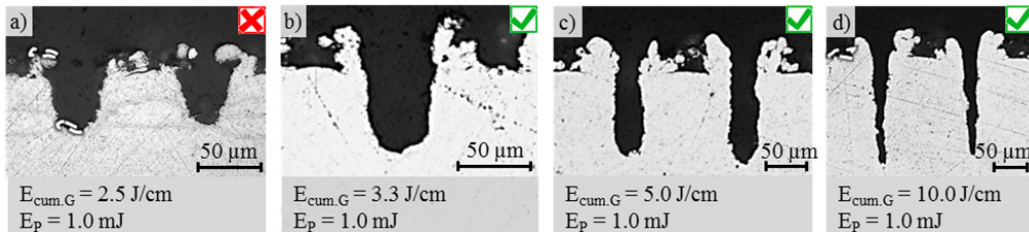


Fig. 12. Cross section images of groove structures with helium leakage (a) and gas-tight joints (b, c and d) with air pockets.

### 3.3. Mechanical strength of the hybrid joints

The results of the mechanical test before and after the climate change are shown in Fig. 13. Only gas-tight processing parameters were used for the analysis.

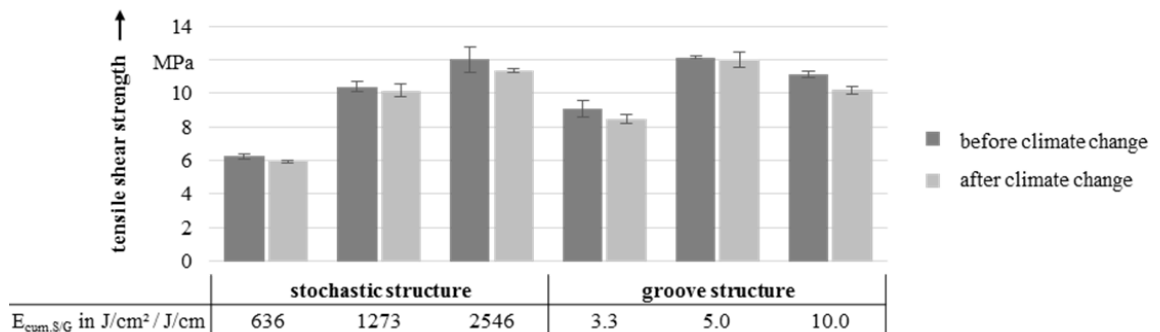


Fig. 13. Tensile shear strength for stochastic and groove structures before and after climate change tests.

For the stochastic structures the tensile shear strength correlates with the cumulative energy and in consequence with the surface roughness. A maximum joint strength of 12.0 MPa was achieved at an energy of 2546 J/cm².

Increasing the surface roughness and size led to enhanced mechanical interlocking between the PP and the pre-treated AL surface. In addition, it is assumed that the formation of a thick porous oxide increases the specific adhesion which causes a higher joint strength (Kurtovic 2014). After the climate change tests all specimens with a stochastic structure exhibited a slightly decreased tensile shear strength. The joint strength was by up to 0.6 MPa lower at a cumulative energy of 2546 J/cm<sup>2</sup>.

The specimens with the groove structures exhibited the highest joint strength for 5.0 J/cm. Lower groove depths which resulted from energies at 3.3 J/cm led to a decrease in joint strength. The grooves manufactured with 10.0 J/cm exhibited an increased groove depth of up to 217 µm and equal groove widths in comparison to 5.0 J/cm. However, a slight decrease in joint strength from 5.0 J/cm to 10.0 J/cm was observed. It is believed that the particularly formed burrs at 5.0 J/cm showing an undercut led to enhanced mechanical interlocking and in consequence to the highest shear strengths (Fig. 8 d). Similar to the stochastic structures, the tensile shear strength decreased after the climate change test by up to 0.9 MPa. In Amend et al. (2013) a comparable climate change test was performed with similar groove structures but polyamide instead of PP. This led to a halving in mechanical strength. The authors came to the conclusion that the decrease was most likely caused by physical and chemical aging of the thermoplastic. The low decrease in the current study may be explained since PP is known for a low permeability to water as well as a good chemical stability and is therefore less susceptible to aging and the climate change test.

#### 4. Summary and conclusions

- AL specimens were pre-treated by pulsed laser radiation manufacturing stochastic and groove structures. Subsequently, laser based thermal heat conduction joining was applied to bond the AL with the PP in order to create gas-tight joints.
- The microscopic roughness of the stochastic structures correlates with the cumulative laser energy applied. In addition, a porous oxide layer is generated which thickens at the same time. High levels of cumulative energy and surface roughness caused the formation of isolated air pockets in the joint region. Gas-tightness of the hybrid joints with a stochastic structure was measured before and after a climate change test for a cumulative energy of more than 636 J/cm<sup>2</sup> and 1.0 mJ pulse energy. Less energy led to a leakage in the test and an insufficient bonding of the PP after the climate changes with a low mechanical strength.
- The groove structures exhibit a formation of burr with an increase in the cumulative energy. The groove depth correlates linearly to the cumulative energy for both pulse energies of 0.5 mJ and 1.0 mJ, respectively. However, the groove width is mainly influenced by both the pulse and the cumulative energy. Low pulse energies or high cumulative energies cause melt residues inside the grooves. Groove structures with a cumulative energy of more than 3.3 J/cm at a pulse energy of 1.0 mJ could be identified as gas-tight. Due to low groove widths, incomplete infiltration and the formation of air pockets, leakage was observed when using a pulse energy of 0.5 mJ.
- A tensile shear strength of up to 12.0 MPa was achieved for both laser structures. After climate change, the joint strength of all specimens was slightly decreased (by max. 0.9 MPa) which is believed to be caused by the aging of the thermoplastic.

#### References

- Amend, P.; Pfindel, S.; Schmidt, M., 2013. Thermal joining of thermoplastic metal hybrids by means of mono- and polychromatic radiation. In: *Physics Procedia* 41, pp. 98-105.
- Amend, P.; Mohr, C.; Roth, S., 2014. Experimental Investigations of Thermal Joining of Polyamide Aluminum Hybrids Using a Combination of Mono- and Polychromatic Radiation. In: *Physics Procedia* 56, pp. 824–834.
- Cenigaonandia, A., Liébana, F., Lamikiz, A., Echegoyen, Z., 2012. Novel Strategies for Laser Joining of Polyamide and AISI 304. In: *Physics Procedia* 39, pp. 92–99.
- DIN EN 1465:2009, July 2009. Adhesives - Determination of Tensile Lap-Shear Strength of Bonded Assemblies.
- DIN EN 1779:1999, October 1999. Non-destructive testing – Leak testing - Criteria for method and technique selection.
- Heckert, A.; Zaeh, M. F., 2014. Laser Surface Pre-treatment of Aluminium for Hybrid Joints with Glass Fibre Reinforced Thermoplastics. In: *Physics Procedia* 56, pp. 1171–1181.
- Hose, R., 2008. *Laseroberflächenvorbehandlung zur Verbesserung der Adhäsion und Alterungsbeständigkeit von Aluminiumklebungen*. PhD Thesis, Aachen: Shaker Verlag.

- Kawahito, Y., Tange, A., Kubota, S., Katayama, S., 2006. Development of Direct Laser Joining for Metal and Plastic. In: ICALEO 2006 Congress Proceeding, pp. 376–382.
- Kurtovic, A., 2014. Laserinduzierte Nanostrukturierung von Titanoberflächen für das strukturelle Kleben. Einfluss auf die Oberflächenmorphologie, Ermüdungs- und Adhäsionseigenschaften. PhD Thesis, Paderborn: Universitätsbibliothek Paderborn.
- Lamberti, C.; Solchenbach, T.; Plapper, P.; Possart, W., 2014. Laser Assisted Joining of Hybrid Polyamide-aluminum Structures. In: Physics Procedia 56, pp. 845–853.
- Rechner, R., 2012. Laseroberflächenvorbehandlung von Aluminium zur Optimierung der Oxidschichteigenschaften für das strukturelle Kleben. PhD Thesis, 1st Edition. München: Dr. Hut.
- Rodríguez-Vidal, E.; Lambarri, J.; Soriano, C.; Sanz, C.; Verhaeghe, G., 2014. A combined experimental and numerical approach to the laser joining of hybrid Polymer – Metal parts. In: Physics Procedia 56, pp. 835-844.
- Roesner, A., 2014. Laserbasiertes Fügeverfahren zur Herstellung von Kunststoff-Metall-Hybridbauteilen. PhD Thesis, Stuttgart: Fraunhofer Verlag.
- Saechtling, H.; Baur, E., 2007. Saechtling-Kunststoff-Taschenbuch. München: Hanser.
- Schricker, K.; Stambke, M.; Bergmann, J.P., 2015. Adjustment and Impact of the Thermoplastic Microstructure of the Melting Layer in Laser-based Joining of Polymers to Metals. In: Wissenschaftliche Gesellschaft Lasertechnik e.V (Ed.). Lasers in Manufacturing 2015 (LIM 2015), München.
- Spadaro, C.; Sunseri, C.; Dispenza, C., 2007. Laser surface treatments for adhesion improvement of aluminium alloys structural joints. In: Radiation Physics and Chemistry 76 (8-9), pp. 1441–1446.